Facile template-free synthesis of uniform V_2O_3 hollow microspheres for stable and fast lithium storage

Chunhua Han, Fang Liu, Jinshuai Liu, Qi Li, Jiashen Meng, Bowen Shao, Qiu He, Xuanpeng Wang, Ziang Liu, Liqiang Mai**

State Key Laboratory of Advanced Technology for Materials Synthesis and Processing, Wuhan University of Technology, Wuhan 430070, China

**Email - mlq518@whut.edu.cn, mlq518@163.com*

Experimental

Synthesis of uniform V_2O_3@NC hollow microspheres

All the reagents are of analytical grade and used as-received without further purification. First, 0.5 g of vanadium acetylacetonate and 1 g of 2-dimethylimidazole were successively dissolved in 40 mL of N, N-dimethylformamide (DMF) solvent under stirring. The resulting mixture was stirred for another 1 h at room temperature. The obtained solution was transferred to a 50 mL Teflon autoclave and then heated to 160 °C for 12 h. Then, the V-2-MIM complex precursor hollow microspheres were collected, washed with ethyl alcohol three times and dried under vacuum at 60 °C for 12 h. Subsequently, after sintered at 500 °C for 3 h in argon, uniform V_2O_3@NC hollow microspheres were obtained.

Characterizations

The crystallographic characteristics of the final products were measured using a Bruker D8 Discover X-ray diffractometer equipped with a Cu Kα radiation source. Scanning electron microscopy (SEM) images were collected by a JEOL JSM-7100F at an acceleration voltage of 15 kV. TEM images were collected using a JEM-2100F transmission electron microscope. Energy-dispersive X-ray spectra were recorded using an Oxford IE250 system. Raman and FTIR spectra were obtained using a Renishaw INVIA micro-Raman spectroscopy system. X-ray photoelectron spectroscopy (XPS) measurements were conducted using a VG MultiLab 2000 instrument. The Brunauer-Emmett-Teller (BET) surface areas and pore size distribution were measured using Tristar II 3020 instrument by nitrogen adsorption at 77 K. TG-DSC analysis was conducted using an STA-449F3 instrument. ICP-AES analysis was conducted using a Prodigy 7 instrument.

Electrochemical measurements

The working electrode slurry was composed of 70 wt% V_2O_3@NC hollow microspheres, 20 wt% acetylene black, 10 wt% polyvinylidene fluorides (PVDF) and N-methyl-2-pyrrolidinone (NMP). After coating onto copper foil, the electrode film was uniformly cut into~0.5 cm^2 (area) round slices, weighing a total of ~ 1.0 mg; the corresponding areal mass loading was 2 mg cm^{-2}. Cell assembly was carried out in an argon-filled glove box with the concentrations of moisture and oxygen below 0.1 ppm. Lithium foil was used as the counter electrode and the separator was Celgard 2400 microporous membrane. 1 M lithium hexafluorophosphate ($LiPF_6$) solution in ethylene carbon (EC)-dimethyl carbonate (DMC) (1:1 v/v) was used as the electrolyte. Galvanostatic charge/discharge measurements were performed using a multichannel battery testing system (LAND CT2001A). Cyclic voltammetry (CV) and electrochemical impedance spectroscopy (EIS) were performed with a CHI 600e electrochemical workstation and Auto lab PGSTAT 302N.

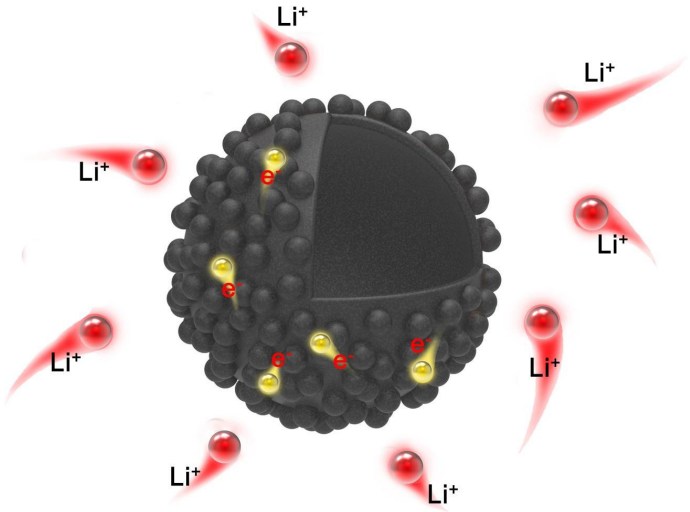

Fig. S1 Schematic illustration of single V_2O_3@NC hollow microsphere with efficient electron and Li^+ transport.

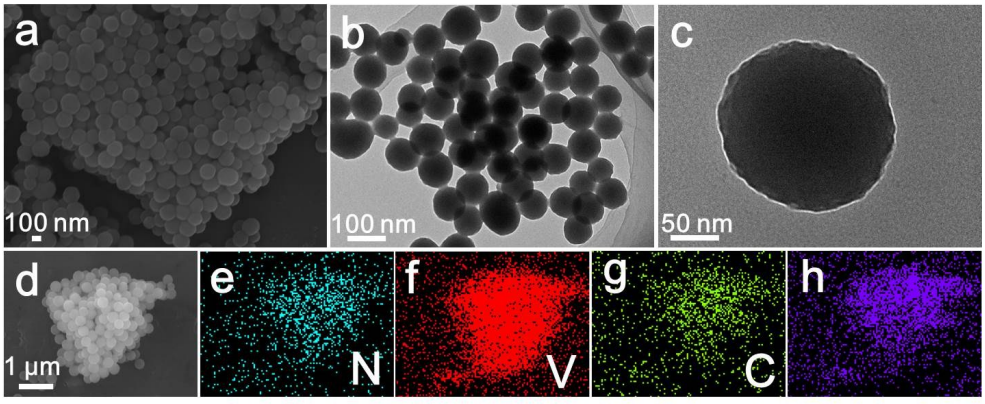

Fig. S2 Characterizations of the V-2-MIM complex solid microspheres. (a) SEM image. (b, c) TEM images. (d-h) SEM image and the corresponding EDS mapping images.

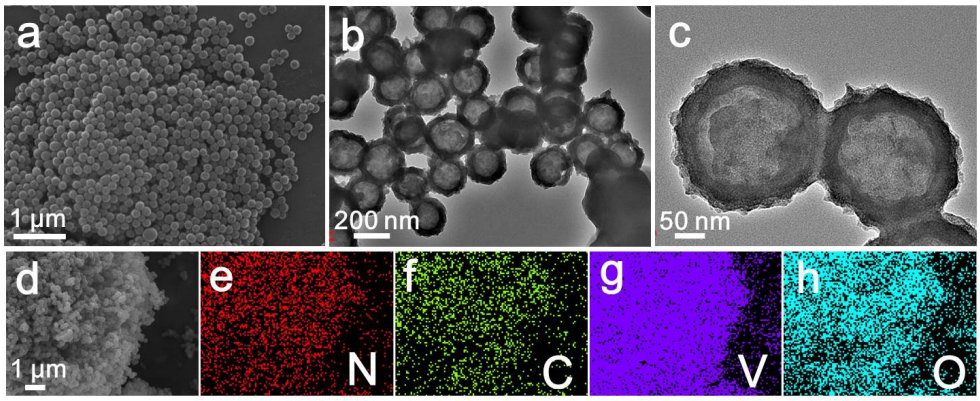

Fig. S3 Characterizations of the V-2-MIM complex yolk-shell microspheres. (a) SEM image. (b, c) TEM images. (d-h) SEM image and the corresponding EDS mapping images.

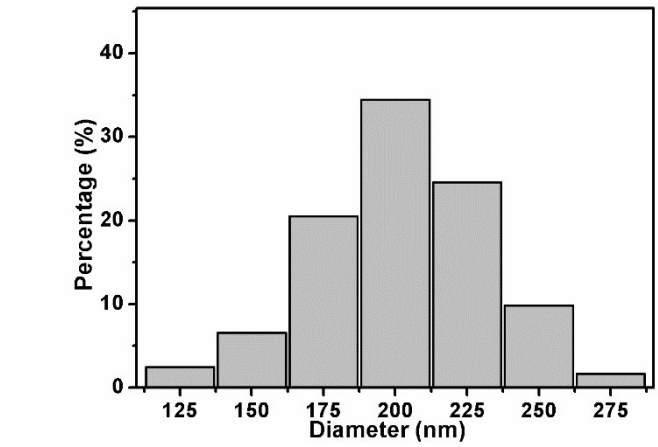

Fig. S4 Diameter distribution of amorphous V-2-MIM complex hollow spheres.

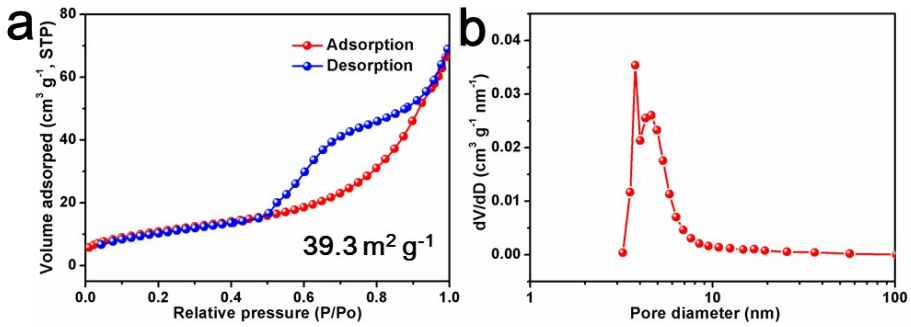

Fig. S5 (a, b) BET and BJH curves of the V-2-MIM complex hollow microspheres.

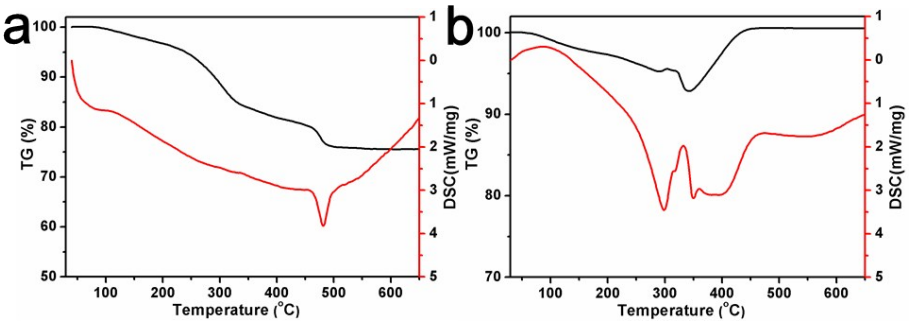

Fig. S6 (a, b) TG and DSC curves of the V-2-MIM complex hollow microspheres tested in argon and air conditions, respectively.

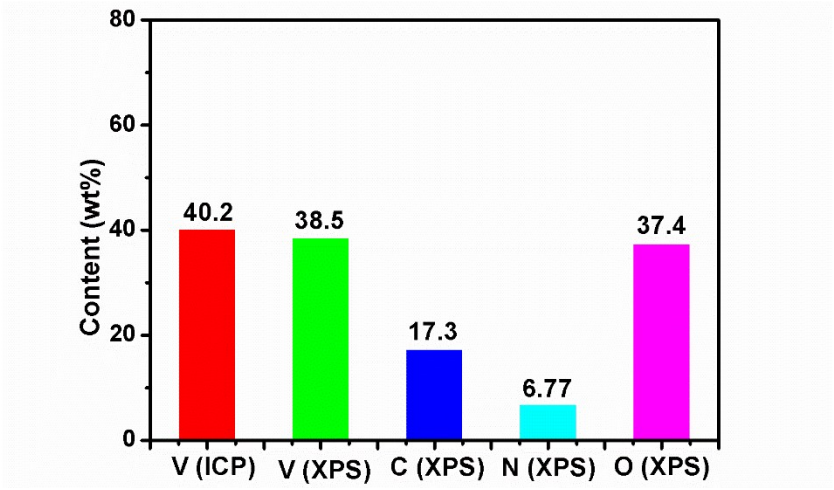

Fig. S7 Elemental content of amorphous V-2-MIM complex hollow spheres, obtained from XPS and ICP-AES measurements.

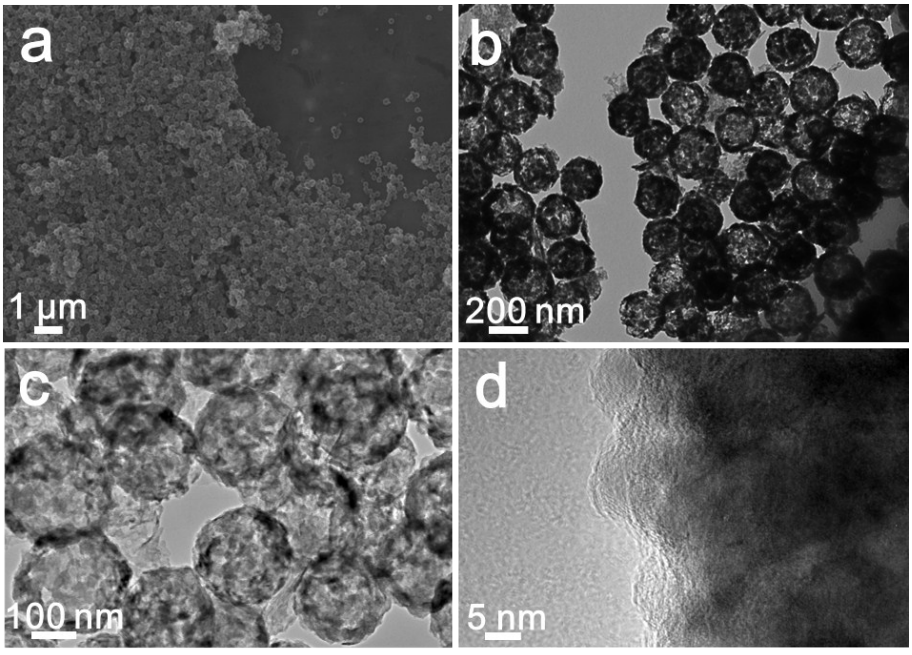

Fig. S8 Morphology characterizations of uniform V_2O_3@NC hollow microspheres. (a) SEM image. (b, c) TEM images. (d) HRTEM image.

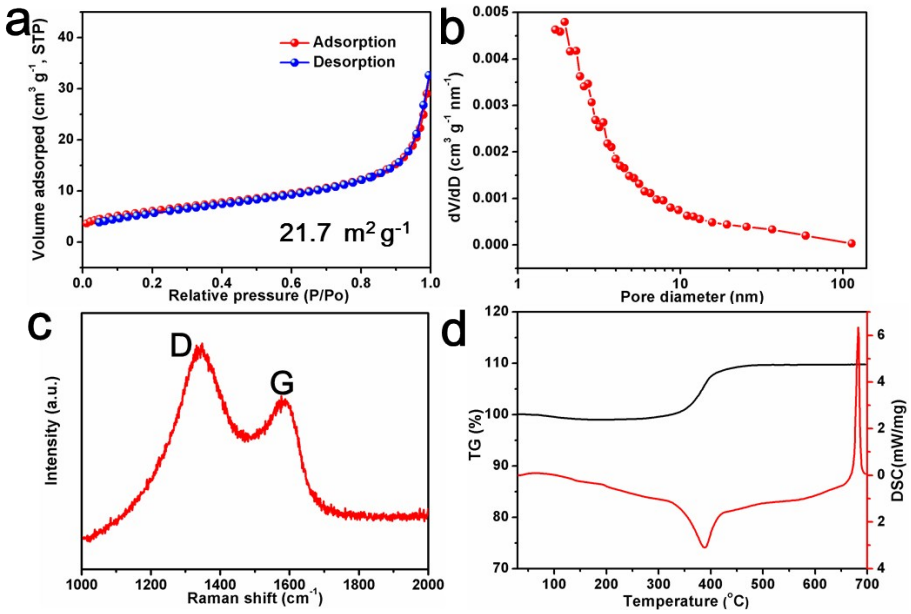

Fig. S9 Structure characterizations of uniform V_2O_3@NC hollow microspheres. (a) BET curve. (b) BJH curve. (c) Raman spectrum. (d) TG and DSC curves.

The reaction equations of V_2O_3@NC hollow spheres during the heat treatment at are as follows:

$$V_2O_3\ (solid) + O_2\ (gas) \rightarrow V_2O_5\ (solid)$$

$$NC\ (solid) + (1+x/2)O_2\ (gas) \rightarrow CO_2\ (gas) + NO_x\ (gas)$$

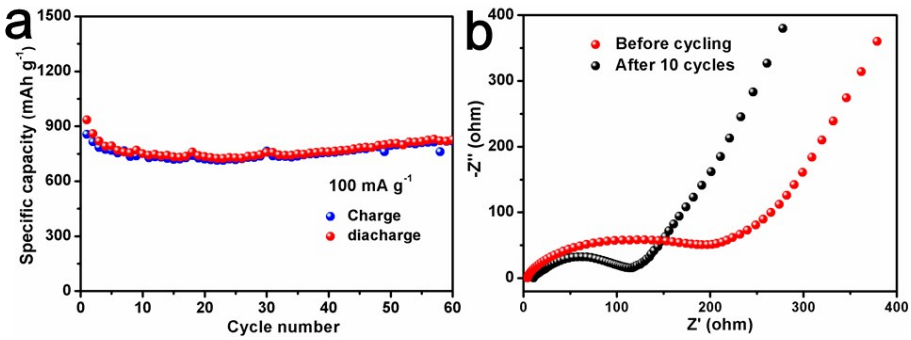

Fig. S10 (a) Cycling performance of V_2O_3@NC hollow microspheres at a current density of 100 mA g^{-1}. (b) The Nyquist plots of V_2O_3@NC hollow microspheres at different cycles.

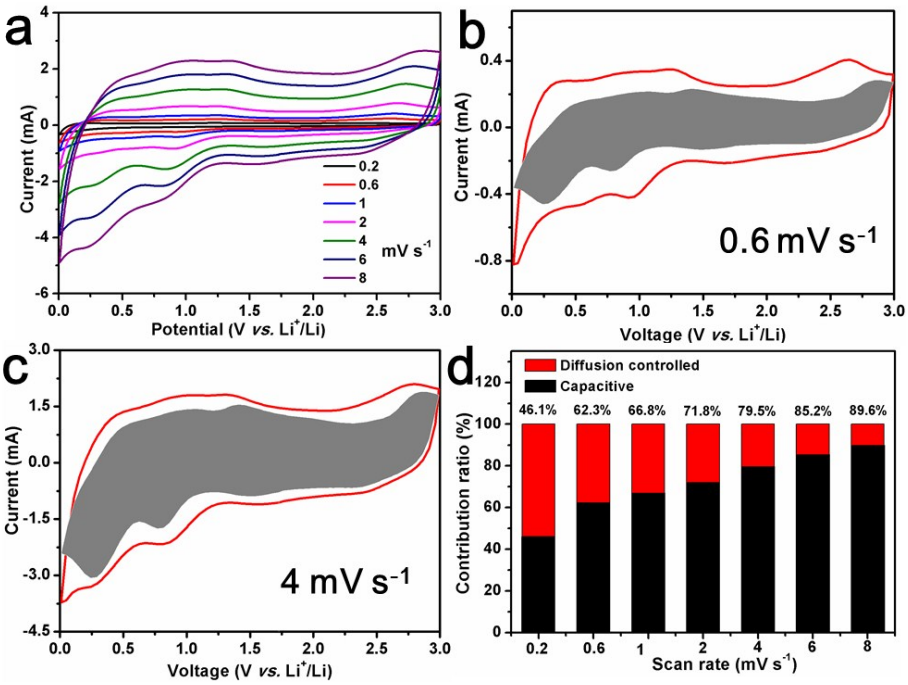

Fig. S11 Lithium storage kinetic analyses of uniform V_2O_3@NC hollow microspheres. (a) CV curves at different scan rates. (b, c) Separation of the capacitive and diffusion currents at scan rates of 0.6 and 4 mV s^{-1}, respectively. (d) Contribution ratio of the capacitive and diffusion-controlled charge versus scan rate.

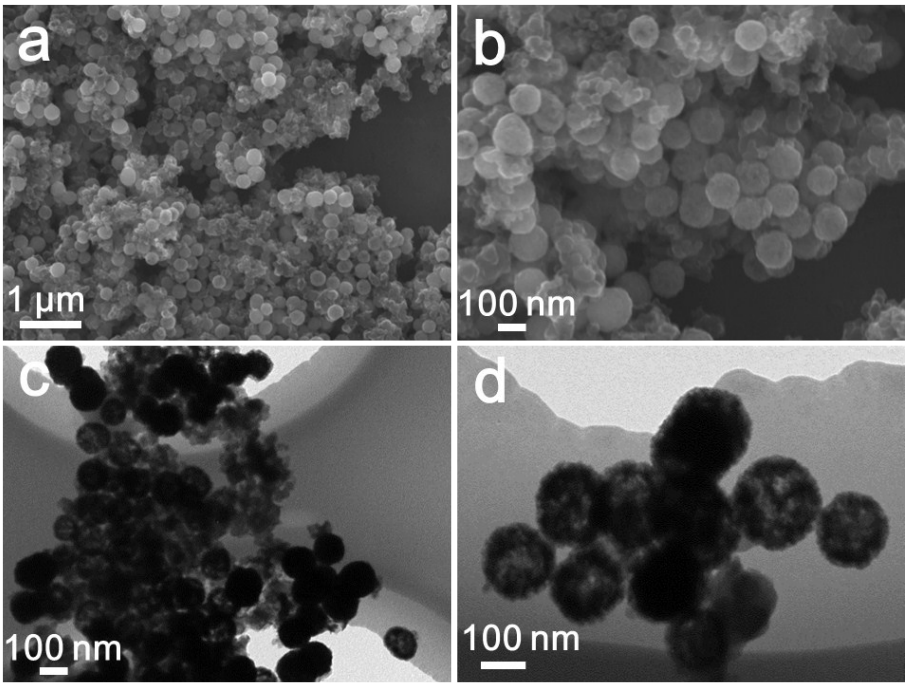

Fig. S12 SEM images (a, b) and TEM images (c, d) of uniform V_2O_3@NC hollow microspheres after 50 cycles at 200 mA g^{-1}.

Table S1. A comparison of our work and previous reports on different carbon-based V_2O_3 nanostructures for LIBs.

Morphology	Voltage range (V)	Current density (mA g^{-1})	Cycle number	Residual capacity (mAh g^{-1})	Capacity retention	Reference
V_2O_3@NC hollow microspheres	0.01-3	200 2000	120 700	811 472	108% 123%	Our work
Coherent porous V_2O_3/carbon nanocomposites	0.01-3	100	200	587	65.9%	Ref. 30
V_2O_3/carbon nano-felts	0.01-3	200	100	420	101%	Ref. 31
Carbon-coated yolk-shell V_2O_3 microspheres	0.01-3	100	100	437.5	92.5%	Ref. 32
Carbon-supported V_2O_3 microspheres	0.01-3	200 2000	600 7000	505 250	194% 100%	Ref. 33
V_2O_3-ordered mesoporous carbon composites	0.02-3	100	180	536	78.2%	Ref. 35
Reduced graphene oxide modified V_2O_3	0.01-3	100 500	50 250	380 270	81.8% 84.3%	Ref. 36